Polymer–agro-waste composites for removal of Congo red dye from wastewater: adsorption isotherms and kinetics

Renuka R. Gonte[a], Gauri Shelar[b], K. Balasubramanian[a],*

[a]*Department of Materials Engineering, Defence Institute of Advanced Technology (DU), Girinagar, Pune 411025, India*
Tel. 0091 20 24389680; Fax: 0091 20 24389411; email: balask@diat.ac.in
[b]*Department of Chemistry, Fergusson College, F C Road, Pune 411004, India*

ABSTRACT

Composites of sawdust and sugarcane molasses with styrene-maleic acid copolymer [(SD-SMA) and (SM-SMA)] were successfully synthesized by suspension polymerization and used as adsorbents for removal of Congo red (CR) dye from aqueous solution. The surface morphology of composite beads was observed under scanning electron microscope, which revealed highly porous surface. Maximum 20 wt.% sawdust and 10 wt.% sugarcane molasses loading were achieved in respective composite. Adsorption of CR was performed in batch process. The effect of initial solution concentration, amount of composite dose, and biomaterial content into the composite were investigated to test the adsorption efficiency and adsorption capacity of these composite beads at pH 7. Adsorption efficiency of 90 and 48% was observed in 2 h using SM-SMA and SD-SMA composites, respectively. The equilibrium data was analyzed using Langmuir, Freundlich, Temkin, and Dubinin–Radushkevich isotherm models. Adsorption onto SD-SMA composites followed the Langmuir model whereas Freundlich model was obeyed by SM-SMA composite beads. Pseudo-second-order kinetics was followed by both types of composites with good correlation coefficient values. The results indicates that SD-SMA and SM-SMA composite beads can be considered as potential adsorbent for the CR dye removal from aqueous solutions.

Keywords: Polymer composite; Agro-waste; SMA; Congo red; Physisorption

1. Introduction

Dyes symbolize colored chemicals used in numerous industries such as textiles, leather, paper, plastic, etc. Colored wastewater is a direct consequence of dye production, use, and inability to remove during coagulation processes. Majority of dyes are synthetic in nature, usually composed of aromatic rings [1], which make them carcinogenic and mutagenic, inert and non-biodegradable when discharged into waste streams, and known to exert potent acute and/or chronic effects on exposed organisms. The water soluble dyes also absorb/reflect sunlight and can inhibit the growth of bacteria. Moreover, are easily visible, resulting in esthetic contamination even at low concentrations [2]. As such, removal of color from aquatic systems has gained significant importance [3,4].

*Corresponding author.

Congo red (CR), a benzidine-based azo dye was selected for the study due to its complex chemical structure and high solubility in aqueous solution. CR metabolizes to benzidine, a known human carcinogen and exposure of which can cause allergic responses. CR is observed in the wastewater discharged (up to 15%) from various dyeing industries [5] and during dyeing operation. Amongst the numerous methods for removal of CR molecules, the treatment methods are divided into three major categories such as: (1) physical methods (adsorption) [6–8]; (2) chemical methods (ozonation [9,10], photo degradation [11] and electrochemical process [12]); and (3) biodegradation [13]. Coagulation, electrocoagulation, flotation, chemical oxidation, filtration, ozonation, membrane separation, ion-exchange, aerobic, and anaerobic microbial degradation are the few methods employed for removal of dye from wastewaters. Selection of the wastewater treatment method is based on the concentration of waste and the cost of treatment. However, these processes have significant disadvantages such as incomplete dye removal, particularly at low concentrations, and high operational costs [14]. Although chemical and biological methods are effective for removing dyes, they involve specialized equipment which are energy intensive and also lead to production of large amounts of by-products [15]. Amongst the several physicochemical processes used for removal of dyes from effluent wastes, adsorption is found to be the most effective [16–18]. Easy regeneration ability, less operational cost, simple design, easy operation, and free or less generation of toxic substances are some of the advantages render by this process [19]. Adsorption process at solid/liquid interface has been extensively employed for several reasons, mainly due to its efficiency and economy [20,21]. Physical adsorption because of its low cost, high efficiency, easy handling, wide variety of adsorbents, and high stabilities towards the adsorbents, is the most widely used method. The economical, easily available, and highly effective adsorbents are still needed and developed [22–24]. Waste materials seem to be viable option for dye removal due to their economic and eco-friendly traits, abundance availability, low cost, regeneration of the biosorbent, and possibility of dye recovery. In this connection, special attention have been given to agricultural wastes like orange peel, banana pith, banana peel, plum kernels, apple pomace, wheat straw, sawdust, coir pith, sugarcane bagasse, tea leaves, bamboo dust, etc.

Several studies have shown that numerous low-cost materials have been successfully applied in the removal of dyes from aqueous solution, some of which are coal, fly ash, wood, silica, shale oil ash, Fuller's earths, zeolite, perlite, alunite, clay materials (bentonite, montmorillonite, etc.) activated slag, and agricultural wastes (bagasse pith, maize cob, coconut shell, rice husk, sawdust, etc.) [25–27]. However, only limited application of such data has been directed towards the design of adsorption treatment systems, for example, batch adsorber design [28,29]. Wood and agricultural-based fibers have applications in water purification. Sawdust is one of the cheapest and abundantly available adsorbent consisting of cellulose, hemicelluloses, and lignin, that has the capacity to adsorb and accumulate heavy metals and pigments from waters and wastewaters. The –COOH and –OH functional groups present in sawdust involve chelation, ion exchange, and complexation mechanism [30]. Cellulose constitutes one-third to one-half of the approximately 150 billion tones of organic matter synthesized annually. Hemicellulose is an ill-defined group of carbohydrate, second in quantity to cellulose [31].

Sugarcane molasses, a byproduct from sugarcane industries and an agricultural waste, is also obtained in large quantity at very cheap rates. For each 10 tonnes of sugarcane crushed, a sugar factory produces nearly 3 tonnes of wet molasses. The high moisture content 40–50% is detrimental to its use as a fuel. A typical chemical analysis might be (on a washed and dried basis): Cellulose 45–55%, Hemicelluloses 20–25%, Lignin 18–24%, Ash 1–4%, and Waxes <1%. Bagasse is an extremely inhomogeneous material comprising around 30–40% of "pith" fiber which is derived from the core of the plant and is mainly parenchyma material; and "bast," "rind," or "stem" fibers which comprises the balance and is largely derived from sclerenchyma material. The adsorptive sites present in these sugarcane molasses such as carbonyl, carboxylic, amine, and hydroxyl groups are able to adsorb dyes by ion exchange phenomena or by complexation [32].

In this study, the removal of CR dye from aqueous solution has been investigated using polymer composite of sawdust and sugarcane molasses with styrene maleic acid copolymer. The main objective of the study was to test the adsorption efficiency of these composite beads under atmospheric conditions. The system variables studied, include sorbent dose, wt.% loading of biomaterials into composite, and initial solution concentration of the dye. The equilibrium and kinetic of adsorption at pH 7 was investigated with these two types of composite beads. The Langmuir, Freundlich, Temkin, and Dubinin–Radushkevich (D–R) isotherms models were used to fit the experimental data. The adsorption rates were determined by linearized models at high and low dye concentration.

2. Methods and materials

2.1. Materials

Styrene (Merk) and divinylbenzene (Sigma–Aldrich 80%) were purified with 1 N NaOH prior to use. Azobisisobutyronitrile (AIBN, SAS) and maleic anhydride (Fluka) were recrystallized from chloroform. Methyl isobutyl ketone, NaOH, NaCl, and $MgCl_2$ were obtained from Qualigens and used as received. CR was obtained from Fluka and used without any purification. The details of CR are presented in Table 1. Fine sawdust powder and sugarcane molasses were obtained from local market. These were washed with distilled water to remove the adhering dust and other fine solid particulates and impurities, and dried. These materials were then sieved to obtain homogeneous sized particle in the size range (50–100 μm).

2.2. Preparation of dye solutions

The dye solution was prepared by dissolving 1 g dye in 1,000 mL deionized water and the desired solution concentrations (10, 20, and 40 mg/L) were prepared by dilution of the stock solution. These solutions were mimicked as per the standards from a local dye company in Pune city, Maharashtra, India.

2.3. Synthesis of SD-SMA and SM-SMA composites

The composite of styrene-maleic acid [33] with sawdust and sugarcane molasses, respectively, were synthesized by suspension polymerization. Briefly, homogeneous mixture of organic monomers i.e. styrene, DVB, MAn, and free radical initiator AIBN (0.8 wt.% based on monomers) was prepared using MIBK solvent. The aqueous phase consisting of saturated salt solution (NaCl, $Mg(OH)_2$)) was prepared in

reaction vessel. The two phases were mixed together under inert conditions. Sawdust and sugarcane molasses were washed in distilled water, dried, and sieved. When the gel point was reached at about 70°C, fine sawdust and sugarcane molasses by weight were added to this mixture and stirred at 800 rpm to obtain the composite beads of 300–600 μm. These sawdust composite beads and sugarcane molasses composite beads were then isolated from the aqueous phase and washed continuously with water followed by toluene to remove unreacted monomers, dilute hydrochloric acid for removal of magnesium hydroxide and finally water washed to remove the acid and salts adhering to the surface of the polymer beads.

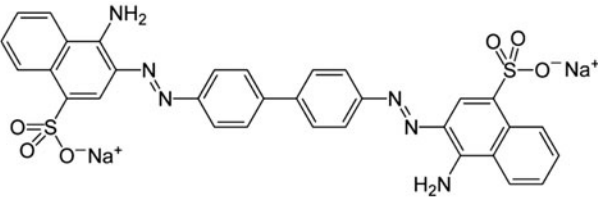### 2.4. Effect of sorbent dose at constant dye concentration

The effect of sorbent dose on the equilibrium uptake of dye ions was investigated with sorbent dose of 0.1, 0.3, and 0.5 g. The experiments were conducted by adding known weights of composite beads to 40 mg/L, 20 mL dye solution at pH 7. The equilibrium concentration of the remaining dye was determined spectrophotometerically. The % adsorption was calculated using formula:

$$\%\text{Ad} = (C_o - C_e)/C_o \times 100 \tag{1}$$

2.5. Effect of initial dye concentrations

Equilibrium uptake of the dye was investigated at 303 K with 0.3 g of composite beads with 10, 20, and 40 mg/L dye solution. The equilibrium concentration of the remaining dye at regular time interval was determined spectrophotometerically.

Table 1
Details of CR dye used for the study

Structure	

IUPAC name	Sodium 3,3′-([1,1′-biphenyl]-4,4′-diyl)bis(4-aminonaphthalene-1-sulfonate)
CAS number	573-58-0
Molecular formula	$C_{32}H_{22}N_6Na_2O_6S_2$
Molar mass	696.665 g/mol

2.6. Effect of biomaterial loading in composite

The effect of wt.% loading of sawdust in SD-SMA composite beads and sugarcane molasses in SM-SMA composite beads was investigated using 40 mg/L dye solution at 303 K. The equilibrium concentration of the remaining dye at regular time interval was determined spectrophotometerically.

2.7. Equilibrium Isotherms

Adsorption isotherm studies were conducted at constant temperature 303 K using 0.3 g composite soaked in 20 mL dye solution for 240 min. Absorbance was observed at regular time interval of 15 min. Adsorption isotherms are plots of equilibrium adsorption capacity (q_e) vs. equilibrium concentration of the residual dye in the solution (C_e). The equilibrium adsorption capacity was calculated using:

$$q_e = (C_o - C_e)/M) \times V \qquad (2)$$

where q_e (mg/g) is the equilibrium adsorption capacity, C_o and C_e the initial and equilibrium concentration (mg/L) of CR in solution, V (L) the volume, and M (g) is the weight of the adsorbent.

2.8. Kinetic studies

Kinetic experiments were conducted by using known weight of composite samples of uniform diameter and different initial CR solution concentrations. Suitable aliquots of the CR solutions with SD-SMA and SM-SMA beads were analyzed for residual concentration of CR present in the solution and recorded at regular time interval of 15 min. The rate constants were calculated by using the conventional rate expression. The amount of metal ion sorbed, q_t, was calculated as:

$$q_t = ((C_o - C_t)/M) \times V \qquad (3)$$

where q_t (mg/g) is the equilibrium adsorption capacity, C_o and C_t the initial and equilibrium concentration (mg/L) of CR solution, V (L) the volume, and M (g) is the weight of the adsorbent.

3. Results and discussion

The synthesized SD-SMA and SM-SMA composite beads were prepared with varying wt.% of biomaterials (5, 10, and 20 wt.%). Addition of sawdust beyond 20 wt.% resulted in encapsulated sawdust particles and no bead formation was observed. Similarly for sugarcane molasses, formation of beads beyond 10 wt.% was not possible. Photographs of SD-SMA and SM-SMA composite beads are shown in Fig. 1.

The study on adsorption of CR dye was carried out at pH 7. CR dye was observed to be chemically and structurally stable at pH 7. Drastic color change was noticed with slight change in pH, hence pH 7 was selected for the study. Similar observations have been reported in the literature [34]. Further, acidic or basic pH affected the adsorbents and it was also observed that solutions with pH 7 were desired in the dye industries.

3.1. Characterization of SD-SMA and SM-SMA composite

The composite beads formed were all in the size range 300–600 μm as observed from the SEM micrographs shown in Fig. 2. It was observed that maximum incorporation of biomaterials into the composite was achieved by addition of biomaterial prior to gel point which resulted in formation of spherical composite beads. The sawdust composite beads obtained were spherical shape while the sugarcane molasses composite beads were elliptical shape. The low magnification SEM micrograph as shown in Fig. 2(a) and (b) confirms the elliptical and spherical shape of SM-SMA and SD-SMA composite beads respectively. The magnified SEM micrographs revealed the porous surface of the formed composites with presence of micropores (1–10 μm). The composite beads possessed hydrophilic nature due to the –COOH group from the organic monomer, lignin, and cellulose content of the biomaterial, and had an affinity towards water, together with these interconnected micropores and rough surface, proved beneficial for diffusion of the dye molecule, which in turn should lead to high adsorption rates.

3.2. Effect of sorbent dose on dye adsorption

Fig. 3(a) and (b) shows the adsorption behavior of CR with different amount of SD-SMA and SM-SMA composite beads. The adsorption efficiency was calculated according to the equation:

$$Ad(\%) = ((C_o - C_t)/C_o) \times 100 \qquad (4)$$

where C_o is the initial conc. of the CR solution, and C_t is the conc. of the CR at time t. For each curve, the Ad increased gradually with time till saturation was achieved. With increase in the SD-SMA adsorbent dose from 0.1 to 0.5 g, the adsorption increased from 15 to 48% and from 35 to 70% with SM-SMA composite. Removal of dye increases with increased adsorbent dosage due to increase in active sites. The
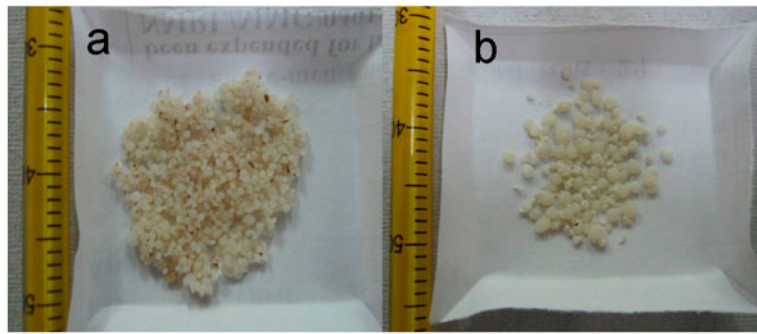
Fig. 1. (a) Spherical SD-SMA; (b) Elliptical SM-SMA composite beads.

difference in the adsorption efficiency in the two composite beads can be attributed to the lignin content, cellulose content, and hemicelluloses content. Since the polar groups present in lignin such as aldehydes, ketones, alcohols, acids, and phenolic hydroxides are involved in the uptake of organic molecule, presence of more functional groups resulted in increase in the efficiency. Further the presence of microtubes in the sugarcane molasses also contributes to this increased adsorption efficiency.

It was observed that the complete decolorization of the CR solution with SD-SMA occurred in 24 h while
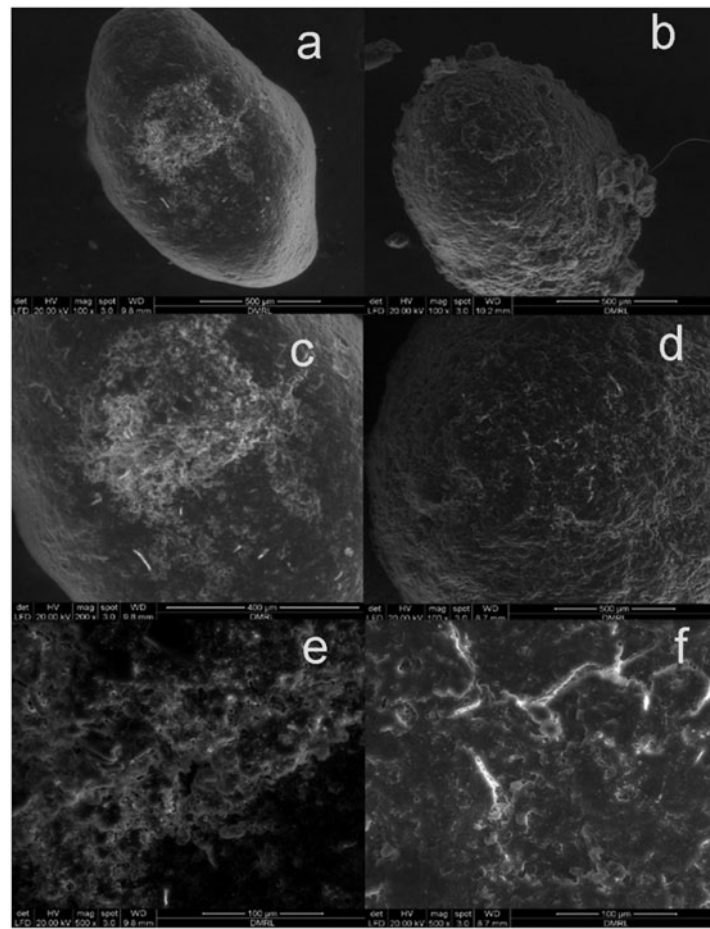

Fig. 2. SEM images (a) SM-SMA; (b) SD-SMA composite bead; magnified surface view of (c and e) SM-SMA and (d and f) SD-SMA.
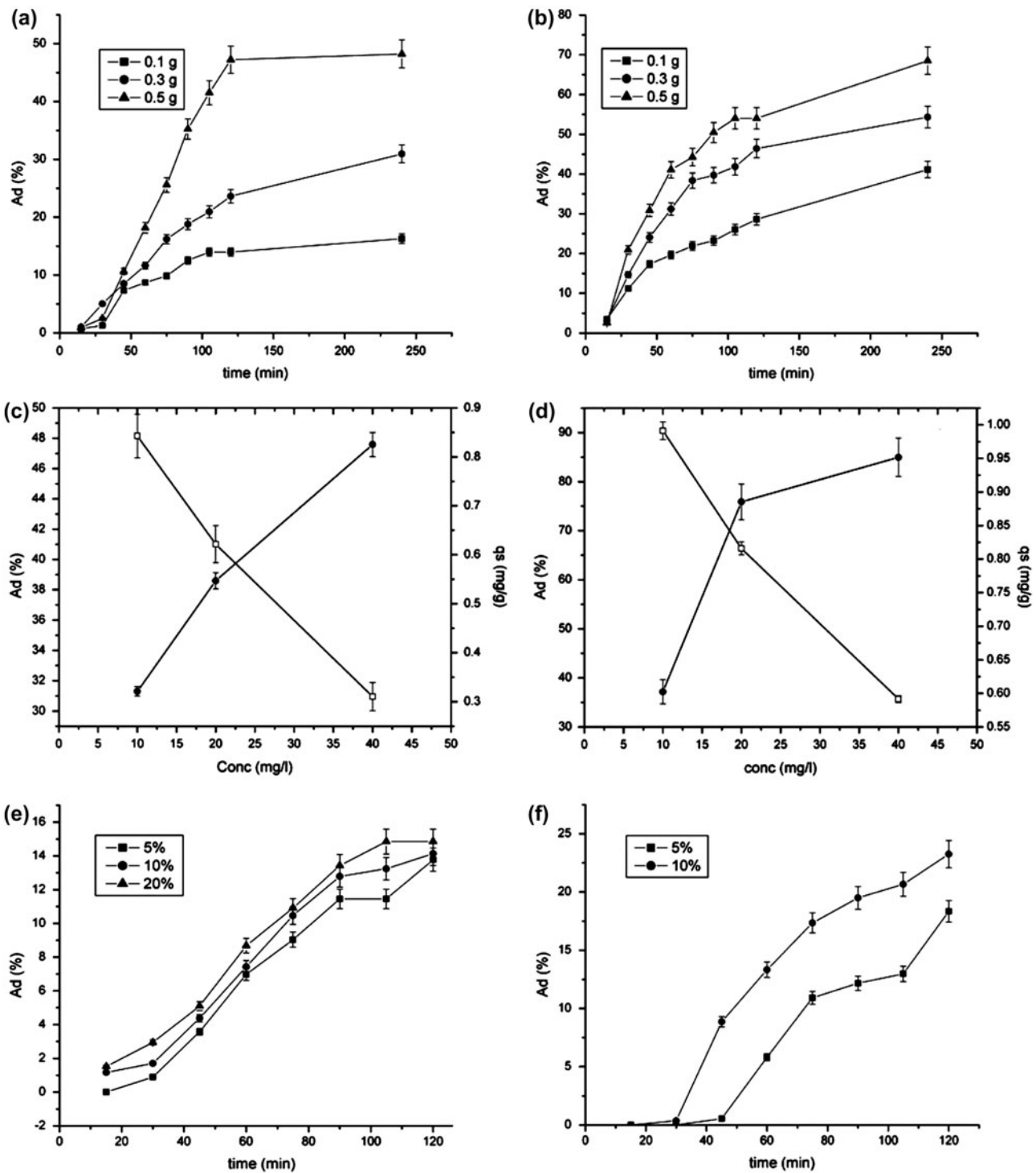
Fig. 3. Effect of adsorbent dose (a) SD-SMA and (b) SM-SMA composite; effect of CR concentration (c) SD-SMA and (d) SM-SMA composite; effect of loading of biomaterial (e) SD-SMA, and (f) SM-SMA composite.

48 h were required for complete decoloration of CR solution of same concentration with SD-SMA composite beads.

3.3. Effect of initial dye concentrations

The effect of CR concentration on the adsorption efficiency and adsorption capacity of the SD-SMA and

SM-SMA composite beads is shown in Fig. 3(c) and (d), respectively. It was observed that increase in the initial dye concentration led to an increase in the adsorption capacity of dye onto composite beads. The adsorption efficiency however decreased from 48 to 30% and 90 to 35% with increase in CR solution concentration. These results indicate that the initial dye concentration played an important role in the adsorption capacity of the CR on the SD-SMA and SM-SMA composite beads. As a rule, increasing the initial dye concentration results in an increase in the adsorption capacity because it provides a driving force to overcome all mass transfer resistances of dyes between the aqueous and solid phase. However, the sorption efficiency decreases since the adsorbent has a limited number of active sites, which becomes saturated at a certain concentration. This indicates that the adsorption capacity will increase with the increase of initial dye concentration mainly due to the rise in the mass transfer from the concentration gradient. However, the concentration will inversely impact on the adsorption efficiency because of the limited adsorption sites available for uptake of dye [35].

3.4. Effect of biomaterial loading in composite beads for adsorption of CR

The effect of increase biomaterial content in the composite on adsorption of CR was investigated with 5, 10, and 20 wt.% of sawdust in SD-SMA and 5 and 10 wt.% sugarcane molasses in SM-SMA composite. Fig 3(e) and (f) shows the adsorption efficiency SD-SMA composite and SM-SMA composite beads with increased wt.% loading of sawdust and molasses respectively. It was observed that with increasing the loading from 5 to 20% of sawdust, no significant change in the adsorption efficiency was observed, however, there was slight increase in Ad, the Ad increased from 13 to 15%. In SM-SMA composite beads however, there was increase in adsorption capacity from 17 to 23% with increasing the loading from 5 to 10 wt.%. This difference in the Ad with different biomaterials is possible due to the increased functional groups and presence of tubular structures in SM-SMA composite.

3.5. Isotherm studies

Adsorption isotherms are important to describe the adsorption mechanism for the interaction of dye on the adsorbent surface for the design of an adsorption process and to determine the efficiency of adsorption. The adsorption isotherm indicates how the adsorption molecules distribute between the liquid phase and the solid phase when the adsorption process reaches an equilibrium state. By plotting solid-phase concentration against the liquid-phase concentration, graphically it is possible to depict the equilibrium isotherm. The analysis of the isotherm data by fitting them to different isotherm models is an important step to find the suitable model that can be used for design purpose. The isotherm thus yields certain constants whose values express the surface properties and affinity of the sorbent. There are several isotherm equations available for analyzing experimental adsorption equilibrium data. Several adsorption isotherms originally used for gas-phase adsorption are available and readily adopted to correlate adsorption equilibria in dye adsorption [35]. Some well-known ones are Freundlich, Langmuir, Tempkin, Redlich–Paterson, Dubinin-Rudushkevich, and Sips equation [36]. In this study, the equilibrium experimental data for adsorbed CR dye onto SD-SMA and SM-SMA composite beads were analyzed using the Langmuir, Freundlich, Tempkin, and Dubinin-Rudushkevich models. The isotherm constants for the four models were obtained by linear regression methods are presented in Table 2.

3.5.1. Langmuir isotherm model

The Langmuir model assumes monomolecular layer formation when adsorption takes place without any interaction between the adsorbed molecules [37]. Langmuir isotherm is applicable to homogeneous sorption where the sorption of each sorbate molecule onto the surface has equal sorption activation energy [38]. The basic assumption of the Langmuir theory is that the uptake of dye occurs on a homogeneous surface by monolayer adsorption without any interaction between the adsorbed ions [39]. The Langmuir model can be represented as:

$$q_e = (q_{max} KLC_e)/(1 + KLC_e) \tag{5}$$

where C_e is the equilibrium concentration (mg/L), qe the amount of CR dye adsorbed (mg/g), q_{max} is q_e for a complete monolayer (mg/g), and KL is a constant related to the affinity of the binding sites (L/mg). The linearized form of the Langmuir equation is:

$$C_e/q_e = 1/(q_{max} KL) + C_e/q_{max} \tag{6}$$

The values of Langmuir constants q_{max} and KL were obtained by linear regression method and shown in Table 2. The essential features of a Langmuir

Table 2
Equilibrium adsorption constants

Adsorption Isotherm		Isotherm parameters	
		SD-SMA	SM-SMA
Langmuir	q_{max} (mg/g)	1.3020	0.9746
	KL	0.0623	1.5857
	RL	0.6166	0.0593
	R^2	0.9997	0.9999
Freundlich	n	1.77	6.97
	KF (mg$1-1/^{n}1^{1/n}$/g)	0.1298	0.6249
	R^2	0.9965	0.9634
Tempkin	B_T (J/mol)	0.3016	0.1100
	a_T (l/min)	0.5453	297.60
	R^2	0.9987	0.9769
Dubinin–Radushkevich	q_{max} (mg/g)	0.8896	0.9265
	$K \times 10^{-6}$	11.09	0.13
	R^2	0.9931	0.9932

isotherm can be expressed in terms of a dimensionless constant separation factor or equilibrium parameter, RL which is defined by Hall et al. [40] as:

$$RL = 1/(1 + KLC_o) \qquad (7)$$

The calculated values of the dimensionless factor RL are included in Table 2. The value of RL provides information as to whether the adsorption is irreversible (RL = 0), favorable (0 < RL < 1), linear favorable (RL = 1) or unfavorable (RL > 1). The RL value obtained for CR with SD-SMA is 0.616 and with SM-SMA is 0.059 which indicate favorable adsorption. The regression coefficient gives good fit to the experimental data for both types of composite beads. This means that the equilibrium isotherms can be well described by the Langmuir model for SM-SMA but describes best the adsorption of CR onto SD-SMA beads confirming monolayer formation.

3.5.2. Freundlich isotherm model

The Freundlich isotherm theory states that the ratio of the amount of solute adsorbed onto a given mass of sorbent to the concentration of solute in the solution is not constant at different concentrations. The heat of adsorption decreases in magnitude with

increasing the extent of adsorption [41]. The Freundlich isotherm is an empirical equation assuming that the adsorption process takes place on heterogeneous surfaces and adsorption capacity is related to the concentration of dye at equilibrium. This isotherm model is defined by the equation [42] below:

$$q_e = KF\,(C_e)^n \qquad (8)$$

where q_e, and C_e are the equilibrium concentrations of dye in the adsorbent (mg/g) and liquid phases (mg/L), respectively, KF and n are the Freundlich constants which are related to adsorption capacity and intensity respectively. This equation can be written in the linear form given below:

$$\ln q_e = 1/n \ln C_e + \ln KF \qquad (9)$$

To determine the maximum sorption capacity, it is necessary to operate with constant initial concentration C_0 and variable weights of sorbent, thus $\ln q_m$ is the extrapolated value of $\ln q$ for $C = C_o$ [37]. According to Halsey [43], the linear plot of $\ln q_e$ vs. $\ln C_e$ gives slope of value $1/n$ and an intercept $\ln KF$. When C_e equals unity $\ln KF$ is equal to $\ln q_e$. In the other case, when $1/n = 1$, the KF value depends on the units in which q_e and C_e are expressed. A favorable adsorption tends to give Freundlich constant n a value between 1 and 10. Larger value of n (smaller value of $1/n$) implies strong interaction between sorbent and metal ions while $1/n$ equal to 1 indicates linear adsorption leading to identical adsorption energies for all the sites. It can be observed from Table 2 that the adsorption of CR onto SD-SMA and SM-SMA composite beads yields positive value of n (1.77 and 6.97 for SD-SMA and SM-SMA, respectively) indicating strong interactions between composite beads and dye. Strong interaction was observed with SM-SMA beads. The high values for the regression coefficients obtained for both the composite beads clearly indicate that the equilibrium adsorption isotherm can be very well described by the Freundlich model.

3.5.3. Temkin isotherm model

Temkin isotherm, considers the effects of the heat of adsorption that decreases linearly with coverage of the adsorbate and adsorbent interactions. [44]. It assumes that the heat of adsorption of all the molecules in the layer decreases linearly with the coverage of molecules due to the adsorbate–adsorbate repulsions and the adsorption of the adsorbate is uniformly distributed [45] and that the fall in the heat of adsorp-
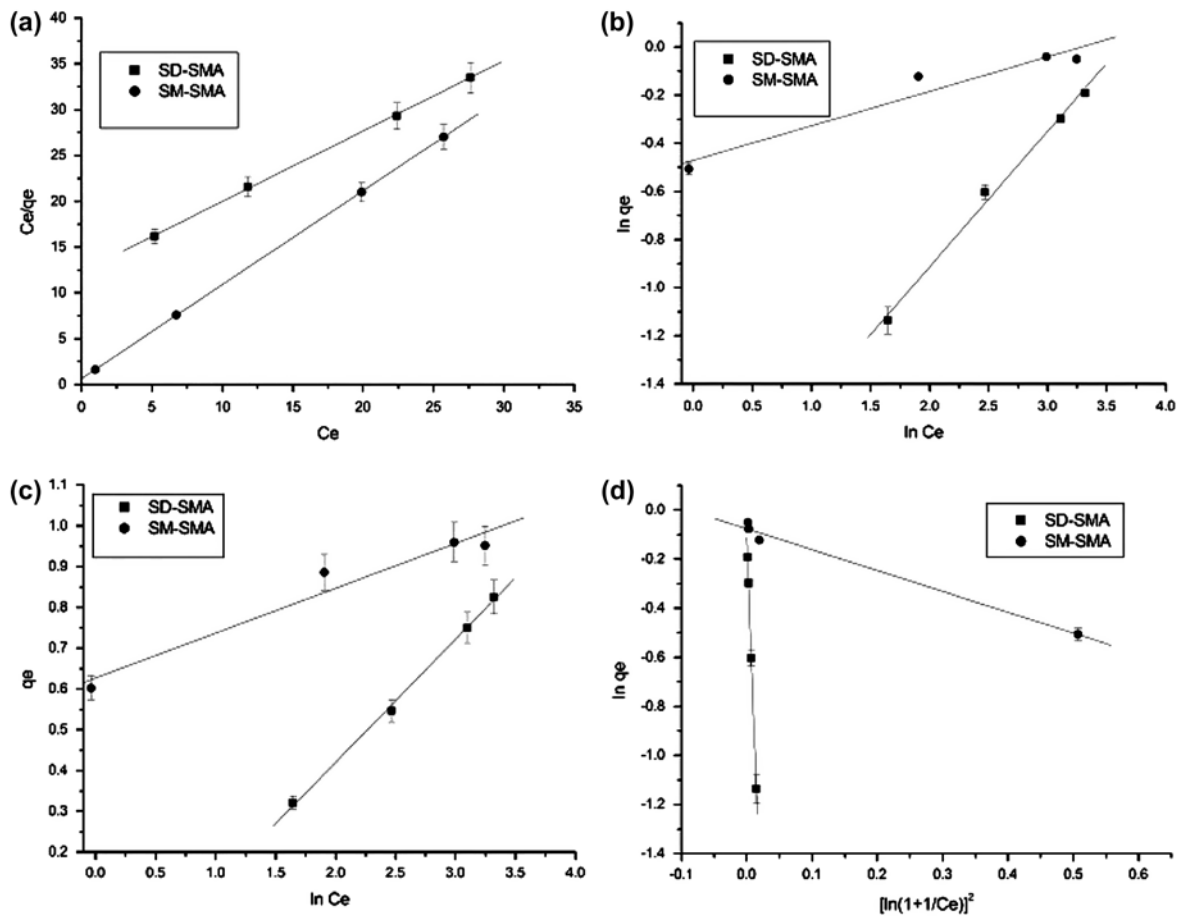
Fig. 4. Equilibrium adsorption isotherm for uptake of CR by SD-SMA and SM-SMA composite (a) Langmuir, (b) Freundlich, (c) Tempkin, and (d) D–R.

tion is linear rather than logarithmic as implied in the Freundlich equation. The Temkin isotherm has been used in the form as follows [46]:

$$q_e = (RT/b_T)\ln(a_T C_e) + (RT/b_T)\ln C_e \tag{10}$$

where R is gas constant $8.314 \times 10^{-3}\,\text{kJ}\,\text{mol}^{-1}\text{K}^{-1}$. T is absolute temperature K, b_T is the Temkin constant related to the heat of adsorption (kJmol^{-1}), and a_T is the equilibrium binding constant corresponding to the maximum binding energy (L/g).

The sorption data can be analyzed according to Eq. (6). The linear plots of q_e vs. $\ln C_e$ enable to determine the constant A_T, B_T, and b_T. Typical bonding energy range for ion exchange mechanism is reported to be in the range of 8–16 kJmol^{-1} while physisorption processes are reported to have adsorption energies less than -40 kJmol^{-1} [47]. The Temkin constants given in Table 2 suggest that the adsorption involves chemisorption and physisorption of the dye molecule.

3.5.4. D–R isotherm

Dubinin [48] proposed the isotherm to estimate the mean free energy of adsorption and is represented in a linear form by equation:

$$\ln q_e = \ln q_{max} - K\varepsilon^2 \tag{11}$$

where K (mol^2 kJ^{-2}) is a constant related to the mean adsorption energy and ε is the Polanyi potential, which can be calculated from equation:

$$\varepsilon = RT\ln(1 + 1/C_e) \tag{12}$$

The plot between $\ln q_e$ and ε^2 at 303 K yields the constant K and q_{max}.

The constant K gives the mean free energy E of sorption per molecule of the sorbate when it is transferred to the surface of the solid from infinity in the solution and can be computed using [49]:

Table 3
Kinetic parameters for adsorption

	C_o (mg/l)	Pseudo-first-order			Pseudo-second-order			Elovich			Intraparticle diffusion	
		q_e	K_1	R^2	q_e	K_2	R^2	σ	$\Theta\sigma$	R^2	Kint	R^2
SD-SMA	10	0.171	2.27×10^{-3}	0.9439	0.207	0.398	0.9995	38.14	11.60	0.9739	22.12	0.8932
	20	0.239	0.0103	0.9939	0.605	0.058	0.9987	12.13	2.70	0.9937	35.52	0.8832
	40	825.2	6.53×10^{-6}	0.9923	1.364	0.005	0.9921	2.41	0.04	0.9962	61.94	0.9306
SM-SMA	10	0.915	0.020	0.9642	1.127	0.004	0.9973	2.39	11.61	0.9739	56.79	0.8662
	20	0.692	0.011	0.9768	1.066	0.016	0.9906	4.98	4.09	0.9350	52.80	0.9621
	40	1.029	0.011	0.9910	1.587	0.004	0.9917	3.14	0.07	0.9900	78.30	0.9666

$$E = 1/\sqrt{2K} \tag{13}$$

The adsorption of CR onto both composite beads fits well with the D–R isotherm with regression coefficient values 0.92 and 0.98, respectively, for SD-SMA and SM-SMA. This suggests that the isotherms could be more appropriate under industrial conditions.

The results indicate that the experimental data fits well with the Langmuir, Freundlich, Temkin, and D–R isotherm models for both SD-SMA and SM-SMA composite beads. Adsorption of CR onto SD-SMA is best represented by Langmuir model whereas Freundlich model best describes the adsorption of CR onto SM-SMA composite beads, indicating adsorption onto heterogeneous surface via physicochemical process involving the –OH, –COOH groups of the composite beads. Fig. 4 presents the equilibrium isotherms displayed by SD-SMA and SM-SMA composite for uptake of CR from aqueous solution and the isotherm constants are mentioned in Table 2.

3.6. Kinetics

The uptake of CR as a function of contact time was tested using different initial concentration of dye. It was observed that the adsorption rate of dye uptake was slow and maximum uptake was achieved within 2 h. Complete uptake of dye occurred in 48 h. To investigate the mechanism of adsorption and its potential rate-controlling steps that include mass transport and chemical reaction processes, kinetic models have been exploited to analyze the experimental data. In addition, information on the kinetics of dye uptake is required to select the optimum condition for full scale batch dye removal processes [35]. Several kinetic models such as pseudo-first-order, pseudo-second-order, Elovich, and intraparticle diffusion have been applied to examine the rate-controlling mechanism of the adsorption process.

3.6.1. Pseudo-first-order kinetic model

Lagergren showed that the rate of adsorption of solute on the adsorbent is based on the adsorption capacity and followed a pseudo-first-order equation which is often used to estimate the k_{ad} considered as mass transfer coefficient in the design calculations. The pseudo-first-order rate equation is given as:

$$\log(q_e - q_t) = \log q_e - (K1/2.303)t \tag{14}$$

where q_e and q_t are the amounts of adsorbed dye on the adsorbent at equilibrium and at time t, respectively (mg/g), and k_1 is the first-order adsorption rate constant (min^{-1}). The plot of log $(q_e - q_t)$ vs. t gives a straight line and the pseudo-first-order rate constant can be calculated from the slope value. The calculated results of the pseudo-first-order rate equation for SD-SMA and SM-SMA composite beads are presented in Table 3. The correlation coefficient values obtained by this method for SD-SMA are in the range 0.91–0.98 which shows good quality of linearization; however, the q_e values acquired by this method do not match with the experimental values. For SM-SMA also though the regression coefficients give a well linear fit, the q_e do not match the experimental values. So the reaction cannot be classified as first order. One suggestion for the differences in experimental and theoretical q_e values is that there is a time lag, possibly due to a boundary layer or external resistance controlling at the beginning of the sorption. This time lag is also difficult to quantify. For this reason, it is necessary to use a trial-and-error method in order to obtain the equilibrium uptake [50].

3.6.2. Pseudo-second-order kinetic model

The pseudo-second-order reaction is greatly influenced by the amount of dye on the adsorbent's surface and the amount of dye adsorbed at equilib-

rium. The rate is directly proportional to the number of active surface sites [51]. The pseudo-second-order equation is given as:

$$t/q_t = 1/(K_2 q_e) + t/q_e \qquad (15)$$

where K_2 is the second-order adsorption rate constant (gm/(g min)), and q_e is the adsorption capacity calculated by the pseudo-second-order kinetic model (mg/g). The constant K_2 is used to calculate the initial sorption rate h (mg/(g min)), at t→0 as follows:

$$h = K_2 q_e \qquad (16)$$

The application of the pseudo-second-order kinetic by plotting t/q_t vs. t yielded the second-order rate constant K_2. The kinetic parameters calculated are shown in Table 3 for SD-SMA and SM-SMA. The calculated q_e

values agreed very well with the experimental data and the correlation coefficient gives best fit linearized plots for both the composite beads. Thus experiment results supports the assumption behind the model that the rate-limiting step in adsorption of CR dye are chemisorptions involving valence forces through the sharing or exchange of electrons between adsorbent and dye molecules.

3.6.3. Elovich model

In reactions involving chemisorption of adsorbate on a solid surface without desorption of products, adsorption rate decreases with time due to an increased surface coverage. One of the most useful models for describing such "activated" chemisorption is the Elovich equation [52]. Elovich equation is a rate equation based on the adsorption capacity describing
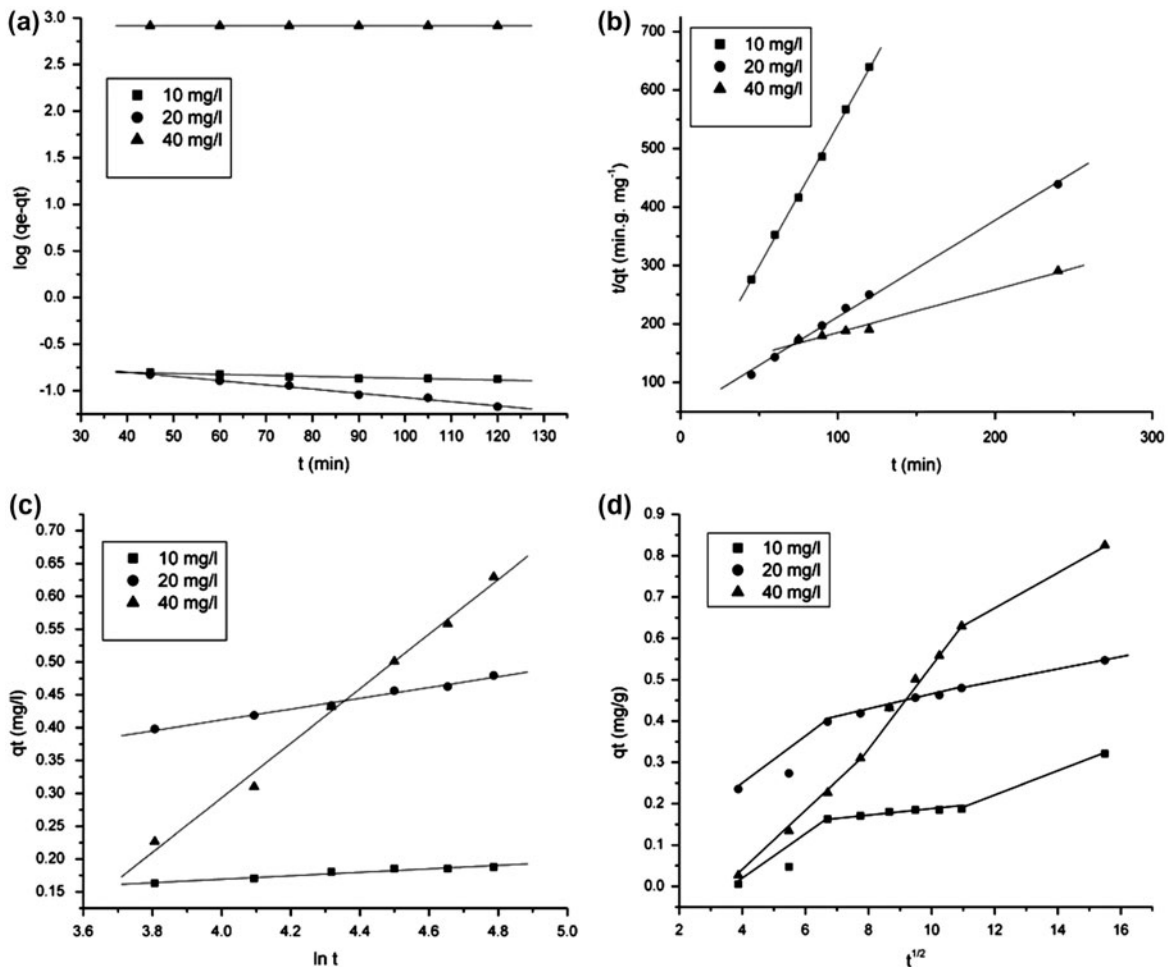

Fig. 5. Kinetic models for uptake of CR using SD-SMA composite (a) pseudo-first-order, (b) pseudo-second-order, (c) Elovich, and (d) intraparticle diffusion.
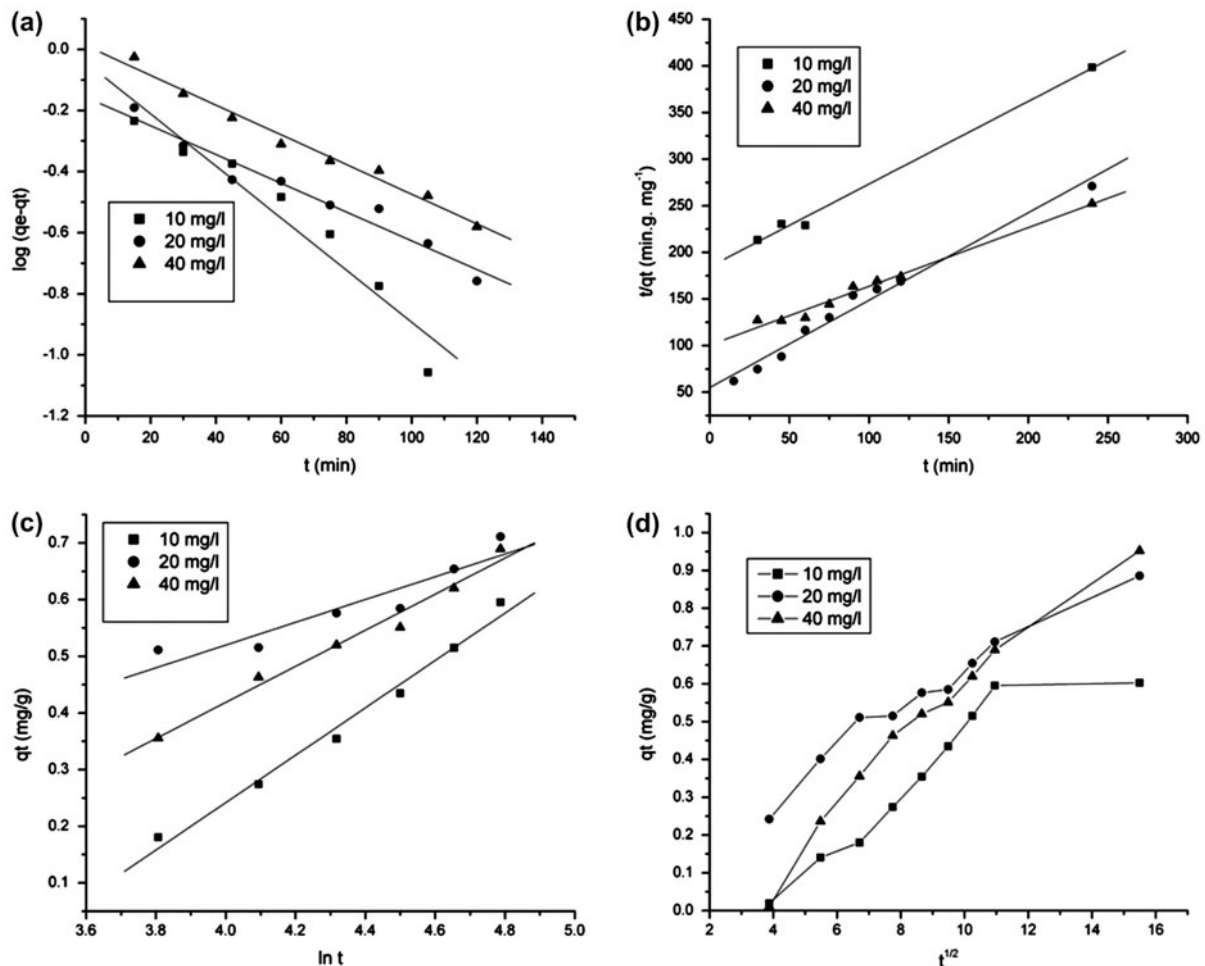
Fig. 6. Kinetic models for uptake of CR using SM-SMA composite (a) pseudo-first-order, (b) pseudo-second-order, (c) Elovich, and (d) intraparticle diffusion.

the adsorption on highly heterogeneous adsorbent which is expressed as [53]:

$$dq_t/dt = \alpha \exp(-\beta q_t) \tag{17}$$

where α $(mg\,g^{-1}\,min^{-1})$ is the initial adsorption rate and β (g/mg) is the desorption constant related to the extent of surface coverage and activation energy for chemisorption. The simplified equation can be given as:

$$q_t = 1/\sigma \ln(\theta\sigma) + 1/\sigma \ln t \tag{18}$$

Assuming $\theta\sigma \gg t$ and $q_t = 0$ at $t = 0$ [53].

The linearized form of Elovich kinetic equation is a plot of q_t vs. $\ln t$ to obtain the kinetic constants. The regression coefficient constants for almost all dye concentration for both the composite beads gives best fit and reveals linear characteristics.

3.6.4. Adsorption mechanism

The prediction of the rate-limiting step is an important factor to be considered in the adsorption process [54]. It is governed by the adsorption mechanism, which is generally required for design mechanism. For a solid–liquid sorption process, the solute transfer is usually characterized by external mass transfer (boundary layer diffusion), or intraparticle diffusion, or both. The most commonly used technique for identifying the mechanism involved in the adsorption process is by fitting and intraparticle diffusion plot. According to Weber and Morris [55], an intraparticle diffusion coefficient k_{id} is given by the equation:

$$q_t = K_{int}\, t^{1/2} \tag{19}$$

where K_{int} is the intraparticle diffusion rate constant $(\mathrm{mg\,g^{-1}\,min^{-0.5}})$. The plot of q_t vs. $t^{1/2}$ at different initial solution concentrations gives the value of Kint and may present multilinearity which indicates two or more steps occurring in the adsorption process. The first sharper portion is the external surface adsorption or instantaneous adsorption stage. The second portion is the gradual adsorption stage where the intraparticle diffusion rate is controlled. The third is the final equilibrium stage where intraparticle diffusion starts to slow down due to extremely low solute concentration in the solution. The intraparticle diffusion rate was obtained from the slope of the gentle-sloped portion. The value of Kint was higher at the higher concentrations. The multi-stepped adsorption observed for CR and best fitting obtained for the experimental data with high regression coefficient values indicates that the intraparticle diffusion might play a significant role in the adsorption of dye onto SD-SMA and SM-SMA composite beads. The three step process indicates the attainment of equilibrium. The kinetic models applied for CR with SD-SMA and SM-SMA composite beads are shown in Figs. 5 and 6, respectively, and the kinetic parameters are compiled in Table 3.

3.7. Thermodynamic studies

Thermodynamic considerations are important to conclude whether the adsorption process is spontaneous or not. The adsorption of CR dye SD-SMA beads and SM-SMA beads was studied at 303 K. The free energy for adsorption ($\Delta G°$) was calculated from the equation [56]:

$$\Delta G° = -RT \ln K_L \tag{20}$$

where K_L is the equilibrium constant obtained from Langmuir isotherm, R is universal gas constant $(8.314\,\mathrm{Jmol^{-1}\,K^{-1}})$ and T is absolute temperature (K). The free energy values obtained for uptake of CR onto SD-SMA and SM-SMA are 6.99 and $-1.16\,\mathrm{kJmol^{-1}}$, respectively. The negative value obtained confirms feasibility and spontaneous nature of adsorption and endothermic adsorption.

4. Conclusion

The abundant agricultural waste/byproducts, sawdust, and sugarcane molasses were used in synthesizing polymer composite for uptake of CR dye from aqueous solution. These were also identified as the cheapest and easily/readily available source for synthesizing composite material with high adsorption capacity. The composites were found to possessed high chemical resistance. Maximum of 20 wt.% sawdust and 10 wt.% molasses could be incorporated in the formation of composite beads. SM-SMA composites exhibited 90% adsorption within 2 h while SD-SMA composites could achieve only 50% adsorption for the same initial solution concentration of the dye, and required 5 h to achieve 90% adsorption. The adsorption capacities were significantly affected by initial dye concentration. Langmuir, Freundlich, Temkin, and D-R isotherm adsorption models were used for the mathematical description of the adsorption equilibrium for both SD/SM-SMA composite beads. The results indicated that adsorption onto SD-SMA followed the Langmuir model whereas adsorption on SM-SMA was best described by the Freundlich model, indicating heterogeneous surface binding and suggesting physicochemical sorption of dye from aqueous solution. The adsorption kinetics indicates good agreement with the pseudo-second-order kinetic model for all different CR concentrations.

References

[1] M.A. Brown, S.C. De Vito, Predicting azo dye toxicity, Crit. Rev. Environ. Sci. Technol. 23 (1993) 249–324.
[2] H. Yu, B. Fugetsu, A novel adsorbent obtained by inserting carbon nanotubes into cavities of diatomite and application for organic dye elimination from contaminated water, J. Hazard. Mater. 177 (2010) 130–145.
[3] A.R. Gregory, S. Elliot, P. Kluge, Ames testing of direct black 3B parallel carcinogenicity, J. Appl. Toxicol. 1 (1991) 308–313.
[4] G. Mckay, M.S. Otterburn, D.A. Aga, Fuller's earth and fired clay as adsorbent for dye stuffs: Equilibrium and rate constants, Water Air Soil Pollut. 24 (1985) 307–322.
[5] R. Han, D. Ding, Y. Xu, W. Zou, Y. Wang, Y. Li, L. Zou, Use of rice husk for adsorption of Congo red from aqueous solution in column mode, Bioresour. Technol. 99 (2008) 2938–2946.
[6] C. Namasivayam, D. Kavitha, Removal of Congo red from water by adsorption onto activated carbon from coir pith, an agricultural solid waste, Dyes Pigm. 54 (2002) 47–58.
[7] I.D. Mall, V.C. Srivastava, N.K. Agarwal, I.M. Mishra, Removal of Congo red from aqueous solution by bagasse fly ash and activated carbon: Kinetic study and equilibrium isotherm analyses, Chemosphere 61 (2005) 492–501.

[8] S. Chatterjee, D.S. Lee, M.W. Lee, S.H. Woo, Enhanced adsorption of Congo red from aqueous solutions by chitosan hydrogel beads impregnated with cetyl trimethyl ammonium bromide, Bioresour. Technol. 100 (2009) 2803–2809.

[9] P. Gharbani, S.M. Tabatabaii, A. Mehrizad, Removal of Congo red from textile wastewater by ozonation, Int. J. Environ. Sci. Technol. 5 (2008) 495–500.

[10] M. Khadhraoui, H. Trabelsi, M. Ksibi, S. Bouguerra, B. Elleuch, Discoloration and detoxification of a Congo red dye solution by means of ozone treatment for a possible water reuse, J. Hazard. Mater. 161 (2009) 974–981.

[11] R.K. Wahi, W.W. Yu, Y. Liu, M.L. Mejia, J.C. Falkner, W. Nolte, V.L. Colvin, Photodegradation of Congo Red catalyzed by nanosized TiO_2, J. Mol. Catal. A-Chem. 242 (2005) 48–56.

[12] M.F. Elahmadi, N. Bensalah, A. Gadri, Treatment of aqueous wastes contaminated with congo red dyes by electrochemical oxidation and ozonation processes, J. Hazard. Mater. 168 (2009) 1163–1169.

[13] K.P. Gopinath, S. Murugesan, J. Abraham, K. Muthukumar, Bacillus sp. Mutant for improved biodegradation of Congo red: random mutagenesis approach, Bioresour. Technol. 100 (2009) 6295–6300.

[14] E. Lorenc-Grabowska, G. Gryglewicz, Adsorption characteristics of Congo red on coal-based mesoporous activated carbon, Dyes Pigm. 74 (2007) 34–40.

[15] T. Robinson, G. McMullan, R. Marchant, P. Nigam, Remediation of dyes in textile effluent: a critical review on current treatment technologies with a proposed alternative, Bioresour. Technol. 77 (2001) 247–255.

[16] N. Nyholm, B.N. Jacobsen, B.M. Pederson, O. Poulsen, A. Damborg, B. Schultz, Removal of organic micro pollutants at ppb levels in laboratory activated-sludge reactors under various operating conditions—Biodegradation, Water Res. 26 (1992) 339–353.

[17] P. Mavros, A.C. Daniilidou, N.K. Lazaridis, L. Stergiou, Color removal from aqueous-solutions, Flotation, Environ. Technol. 15 (1994) 601–616.

[18] D. Ghosh, K.G. Bhattacharyya, Adsorption of methylene blue on kaolinite, Appl. Clay Sci. 20 (2002) 295–300.

[19] E. Khan, M. Li, C.P. Huang, Hazardous waste treatment technologies, Water Environ. Res. 80 (2008) 1654–1708.

[20] C. Namasivayam, R.T. Yamuna, J. Jayanthi, Removal of methylene blue from wastewater by adsorption on cellulose waste, orange peel, Cellul. Chem. Technol. 37 (2003) 333–339.

[21] A. Gurses, C. Dogar, M. Yalcin, M. Acikyildiz, R. Bayrak, S. Karaca, The adsorption kinetics of the cationic dye, methylene blue, onto clay, J. Hazard. Mater. 131 (2006) 217–228.

[22] G. Crini, Non-conventional low-cost adsorbents for dye removal: A review, Bioresour. Technol. 97 (2006) 1061–1085.

[23] V.K. Gupta, Suhas Application of low cost adsorbents for dye removal—A review, J. Environ. Manage. 90 (2009) 2313–2342.

[24] V.K. Gupta, P.J.M. Carrott, M.M.L. Ribeiro Carrott, Suhas Low cost adsorbents: growing approach to wastewater treatment—A review, Crit. Rev. Environ. Sci. Technol. 39 (2009) 783–842.

[25] M. Dogan, M. Alkan, Y. Onguner, Adsorption of methylene blue on perlite from aqueous solutions, Water Air Soil Pollut. 120 (2000) 229–248.

[26] M. Ozacar, I.A. Sengil, A kinetic study of metal complex dye sorption onto pine sawdust, Process Biochem. 40 (2005) 565–572.

[27] G. Annadurai, R.-S. Juang, D.-J. Lee, Use of cellulose-based wastes for adsorption of dyes from aqueous solutions, J. Hazard. Mater. 92 (2002) 263–274.

[28] M. Ozacar, I.A. Sengil, A two stage batch adsorber design for methylene blue removal to minimize contact time, J. Environ. Manage. 80 (2006) 372–379.

[29] O. Demirbas, M. Alkan, M. Dogan, The removal of victoria blue from aqueous solution by adsorption on a low-cost material, Adsorption 8(1) (2002) 341–349.

[30] M. Rafatullah, O. Sulaiman, R. Hashim, A. Ahmad, Adsorption of copper(II), chromium(III), nickel(II) and lead(II) ions from aqueous solutions by meranti sawdust, J. Hazard. Mater. 170 (2009) 969–977.

[31] J.A. Lennox, C. Abriba, Bello N. Alabi, F.C. Akubuenyi, Comparative degradation of sawdust by microorganisms isolated from it, Afr. J. Microbiol. Res. 4(13) (2010) 1352–1355.

[32] A.S. Raymundo, R. Zanarotto, M. Belisario, M. Pereira, J.N. Ribeiro, A.V.F.N. Riberiro, Evaluation of sugarcane bagasses as bioadsorbent in textile wastewater treatment contaminated with carcinogenic congo red dye, Braz. Arch. Biol. Technol. 53 (2010) 931–938.

[33] R. Gonte, K. Balasubramanian, P.C. Deb, P. Singh, Synthesis and characterization of mesoporous hypercrosslinked poly (Styrene Co- Maleic Anhydride) microspheres, Int. J. Polym. Mater. Polym. Biomater. 61(12) (2012) 919–930.

[34] C. Xia, Y. Jing, Y. Jia, D. Yue, J. Ma, X. Yin, Adsorption properties of Congo red from aqueous solution on modified hectorite: Kinetic and thermodynamic studies, Desalination 265 (2011) 81–87.

[35] R. Gonte, K. Balasubramanian, Heavy and toxic metal uptake by mesoporous hypercrosslinked SMA beads: Isotherms and kinetics, J. Saudi Chem. Soc. (in press), doi: http://dx.doi.org/10.1016/j.jscs.2013.04.003.

[36] J. Febrianto, A.N. Kosasih, J. Sunarso, Y.H. Ju, N. Indraswati, S. Ismadji, Equilibrium and kinetic studies in adsorption of heavy metals using biosorbent: A summary of recent studies, J. Hazard. Mater. 162 (2009) 616–645.

[37] Z. Aksu, Determination of the equilibrium, kinetics and thermodynamic parameters of the batch biosorption on nickel (II) ions onto Chlorella vulgaris, Process Biochem. 38 (2002) 89–99.

[38] I. Langmuir, The constitution and fundamental properties of solids and liquids, JACS 38(11) (1916) 2221–2295.

[39] Y. Zhang, Y. Li, X. Li, L. Yang, X. Bai, Z. Ye, L. Zhou, L. Wang, Selective removal of Pb^{2+} in aqueous environment by using novel macroreticular PVA beads, J. Hazard. Mater. 181 (2010) 898–907.

[40] K.R. Hall, L.C. Eagleton, A. Acrivos, T. Vermeulen, Pore and solid diffusion kinetics in fixed bed adsorption under constant—Pattern condition, Ind. Eng. Chem. Fundam. 5 (1996) 212–223.

[41] A. Benhamou, M. Baudu, Z. Derriche, J.P. Basly, Aqueous heavy metal removal on amine functionalized Si-MCM and Si-MCM-48, J. Hazard. Mater. 171 (2009) 1001–1008.

[42] Y.H. Li, Z. Di, J. Ding, D. Wu, Z. Luan, Y. Zhu, Adsorption thermodynamic, kinetic and desorption studies of Pb^{2+} on carbon nanotubes, Water Res. 39 (2005) 605–609.

[43] R. Djeribi, O. Hamdaoui, Sorption of copper (II) from aqueous solution by cedar sawdust and crushed brick, Desalination 225 (2008) 95–112.

[44] G.D. Halsey, The role of surface heterogeneity, Adv. Catal. 4 (1952) 259–269.

[45] K.K.H. Choy, G. McKay, J.F. Porter, Sorption of acid dyes from effluents using activated carbon, Resour. Conserv. Recycl. 27 (1999) 57–71.

[46] P.A. Kumar, M. Ray, S. Chakraborty, Adsorption behaviour of trivalent chromium on the amine-based polymer aniline formaldehyde condensate, Chem. Eng. J. 149 (2009) 115–127.

[47] B. Kiran, A. Kaushik, Chromium binding capacity of Lyngbya putealis exopolysaccarides, Biochem. Eng. J. 38 (2008) 47–54.

[48] B.P. Bering, M.M. Dubinin, V.V. Serpinsky, On thermodynamics of adsorption in micropores, J. Colloid Interface. Sci. 38 (1972) 185–194.

[49] S. Rengaraj, Y. Kim, C.K. Joo, K. Choi, J. Yi, Batch adsorptive removal of copper ions in aqueous solutions by ion exchange resins: 1200H and IRN97H, Korean J. Chem. Eng. 21 (2004) 187–194.

[50] Y. Sag, Y. Aktay, Kinetic studies on sorption of Cr(VI) and Cu(II)ions by chitin, chitosan and Rhizopus arrhizus, Biochem. Eng. J. 12 (2002) 143–153.

[51] S. Rengaraj, J.-W. Yeon, Y. Kim, Y. Jung, Y.-K. Ha, W.-H. Kim, Adsorption characteristics of Cu(II) onto ion exchange resins 252H and 1500H: Kinetics, isotherms and error analysis, J. Hazard. Mater. 143 (2007) 469–477.

[52] A. Gunay, E. Arslankaya, I. Tosun, Lead removal from aqueous solution by natural and pretreated clinoptilolite: Adsorption equilibrium and kinetics, J. Hazard. Mater. 146 (2007) 362–371.

[53] O. Hamdaoui, M. Chiha, Removal of methylene blue from aqueous solutions by wheat bran, Acta Chim. Slov. 54 (2007) 407–418.

[54] M. Sarkar, P.K. Acharya, B. Battacharya, Modeling the adsorption kinetics of some priority organic pollutants in water from diffusion and activation energy parameters, J. Colloid Interface Sci. 266 (2003) 28–32.

[55] W.J. Weber, J.C. Morris, Kinetics of adsorption on carbon from solution, J. Sanit. Eng. Div. Am. Soc. Civ. Eng. 89 (1963) 31–60.

[56] Y.S. Al-Dengs, M.I. El-Barhhouthi, A. El-Shaikh, G. Walker, Effect of solution pH, ionic strength and temperature on adsorption behaviour of reactive dyes on activated carbon, Dyes Pigm. 77(1) (2008) 16–23.